CHAPTER 1

Fundamentals of Impedance Spectroscopy

J. Ross Macdonald[1] **and William B. Johnson**[2]

[1](William R. Kenan, Jr., Professor of Physics, Emeritus), Department of Physics and Astronomy, University of North Carolina, Chapel Hill, NC, USA
[2]W. L. Gore & Associates, Elkton, MD, USA

1.1 BACKGROUND, BASIC DEFINITIONS, AND HISTORY

1.1.1 The Importance of Interfaces

Since the end of World War II, we have witnessed the development of solid-state batteries as rechargeable energy storage devices with high power density; a revolution in high-temperature electrochemical sensors in environmental, industrial, and energy efficiency control; and the introduction of fuel cells to avoid the Carnot inefficiency inherent in noncatalytic energy conversion. The trend away from corrosive aqueous solutions and toward solid-state technology was inevitable in electrochemical energy engineering, if only for convenience and safety in bulk handling. As a consequence, the characterization of systems with solid–solid or solid–liquid interfaces, often involving solid ionic conductors and frequently operating well above room temperature, has become a major concern of electrochemists and materials scientists.

At an interface, physical properties—crystallographic, mechanical, compositional, and, particularly, electrical—change precipitously, and heterogeneous charge distributions (polarizations) reduce the overall electrical conductivity of a system. Proliferation of interfaces is a distinguishing feature of solid-state electrolytic cells, where not only is the junction between electrode and electrolyte considerably more complex than in aqueous cells but also the solid electrolyte is commonly polycrystalline. Each interface will polarize in its unique way when the system is subjected to an applied potential difference. The rate at which a polarized region will change when the applied voltage is reversed is characteristic of the type of interface: slow for chemical reactions at the triple-phase contacts between atmosphere, electrode, and electrolyte, appreciably faster across grain boundaries in the polycrystalline electrolyte. The emphasis in electrochemistry has consequently shifted from a time/concentration dependency to frequency-related phenomena, a trend toward small-signal alternating current (ac) studies. Electrical double layers and their inherent capacitive reactances are characterized by their relaxation times or more realistically by the distribution of their relaxation times. The electrical response of a heterogeneous cell can vary substantially depending on the species of charge present, the microstructure of the electrolyte, and the texture and nature of the electrodes.

Impedance spectroscopy (IS) is a relatively new and powerful method of characterizing many of the electrical properties of materials and their interfaces with electronically conducting electrodes. It may be used to investigate the dynamics of bound or mobile charge in the bulk or interfacial regions of

---

Impedance Spectroscopy: Theory, Experiment, and Applications, Third Edition. Edited by Evgenij Barsoukov and J. Ross Macdonald.

any kind of solid or liquid material: ionic, semiconducting, mixed electronic–ionic, and even insulators (dielectrics). Although we shall primarily concentrate in this monograph on solid electrolyte materials—amorphous, polycrystalline, and single crystal in form—and on solid metallic electrodes, reference will be made, where appropriate, to fused salts and aqueous electrolytes and to liquid metal and high-molarity aqueous electrodes as well. We shall refer to the experimental cell as an electrode–material system. Similarly, although much of the present work will deal with measurements at room temperature and above, a few references to the use of IS well below room temperature will also be included. A list of acronym and model definitions appears at the end of this work.

In this chapter we aim to provide a working background for the practical materials scientist or engineer who wishes to apply IS as a method of analysis without needing to become a knowledgeable electrochemist. In contrast to the subsequent chapters, the emphasis here will be on practical, empirical interpretations of materials problems, based on somewhat oversimplified electrochemical models. We shall thus describe approximate methods of data analysis of IS results for simple solid-state electrolyte situations in this chapter and discuss more detailed methods and analyses later. Although we shall concentrate on intrinsically conductive systems, most of the IS measurement techniques, data presentation methods, and analysis functions and methods discussed herein apply directly to lossy dielectric materials as well.

1.1.2 The Basic Impedance Spectroscopy Experiment

Electrical measurements to evaluate the electrochemical behavior of electrode and/or electrolyte materials are usually made with cells having two identical electrodes applied to the faces of a sample in the form of a cylinder or parallelepiped. However, if devices such as chemical sensors or living cells are investigated, this simple symmetrical geometry is often not feasible. Vacuum, a neutral atmosphere such as argon, or an oxidizing atmosphere is variously used. The general approach is to apply an electrical stimulus (a known voltage or current) to the electrodes and observe the response (the resulting current or voltage). It is virtually always assumed that the properties of the electrode–material system are time invariant and it is one of the basic purposes of IS to determine these properties, their interrelations, and their dependences on such controllable variables as temperature, oxygen partial pressure, applied hydrostatic pressure, and applied static voltage or current bias.

A multitude of fundamental microscopic processes take place throughout the cell when it is electrically stimulated and, in concert, lead to the overall electrical response. These include the transport of electrons through the electronic conductors, the transfer of electrons at the electrode–electrolyte interfaces to or from charged or uncharged atomic species that originate from the cell materials and its atmospheric environment (oxidation or reduction reactions), and the flow of charged atoms or atom agglomerates via defects in the electrolyte. The flow rate of charged particles (current) depends on the ohmic resistance of the electrodes and the electrolyte and on the reaction rates at the electrode–electrolyte interfaces. The flow may be further impeded by band structure anomalies at any grain boundaries present (particularly if second phases are present in these regions) and by point defects in the bulk of all materials. We shall usually assume that the electrode–electrolyte interfaces are perfectly smooth, with a simple crystallographic orientation. In reality of course, they are jagged, full of structural defects and electrical short and open circuits, and they often contain a host of adsorbed and included foreign chemical species that influence the local electric field.

There are three different types of electrical stimuli that are used in IS. First, in transient measurements a step function of voltage [$V(t) = V_0$ for $t > 0$, $V(t) = 0$ for $t < 0$] may be applied at $t = 0$ to the system, and the resulting time-varying current $i(t)$ measured. The ratio $V_0/i(t)$, often called the indicial impedance or the time-varying resistance, measures the impedance resulting from the step function voltage perturbation at the electrochemical interface. This quantity, although easily defined, is not the usual impedance referred to in IS. Rather, such time-varying results are generally Fourier or Laplace transformed into the frequency domain, yielding a frequency-dependent impedance. If a Fourier transform is used, a distortion arising because of the non-periodicity of excitation should be corrected by using windowing. Such transformation is only valid when $|V_0|$ is sufficiently small that system response is linear. The advantages of this approach are that it is experimentally easily accomplished and that the independent variable, voltage, controls the rate of the electrochemical reaction at the interface. Disadvantages include the need to perform integral transformation of the results and the fact that the signal-to-noise ratio differs between different frequencies, so the impedance may not be well determined over the desired frequency range.

Second, a signal $\nu(t)$ composed of random (white) noise may be applied to the interface and measure the resulting current. Again, one generally Fourier transforms the results to pass into the frequency domain and obtain an impedance. This approach offers the advantage of fast data collection because only one signal is applied to the interface for a short time. The technique has the disadvantages of requiring true white noise and then the need to carry out a Fourier analysis. Often a microcomputer is used for both the generation of white noise and the subsequent analysis. Using a sum of well-defined sine waves as excitation instead of white noise offers the advantage of a better signal-to-noise ratio for each desired frequency and the ability to analyze the linearity of system response.

Third, the most common and standard one is to measure impedance by applying a single-frequency voltage or current to the interface and measuring the phase shift and amplitude, or real and imaginary parts, of the resulting current at that frequency using either analog circuit or FFT analysis of the response. Commercial instruments (see Section 3.2) are available, which measure the impedance as a function of frequency automatically in the frequency ranges of about 1 mHz to 1 MHz and which are easily interfaced to laboratory microcomputers. The advantages of this approach are the availability of these instruments and the ease of their use, as well as the fact that the experimentalist can achieve a better signal-to-noise ratio in the frequency range of most interest.

In addition to these three approaches, one can combine them to generate other types of stimuli. The most important of these, ac polarography, combines the first and third techniques by simultaneously applying a linearly varying unipolar transient signal and a much smaller single-frequency sinusoidal signal (Smith [1966]).

Any intrinsic property that influences the conductivity of an electrode–material system, or an external stimulus, can be studied by IS. The parameters derived from an IS spectrum fall generally into two categories: (i) those pertinent only to the material itself, such as conductivity, dielectric constant, mobilities of charges, equilibrium concentrations of the charged species, and bulk generation–recombination rates, and (ii) those pertinent to an electrode–material interface, such as adsorption–reaction rate constants, capacitance of the interface region, and diffusion coefficient of neutral species in the electrode itself.

It is useful and not surprising that modern advances in electronic automation have included IS. Sophisticated automatic experimental equipment has been developed to measure and analyze the frequency response to a small-amplitude ac signal between about 10^{-4} and $>10^{6}$ Hz, interfacing its results to computers and their peripherals (see Section 3.1). A revolution in the automation of an otherwise difficult measuring technique has moved IS out of the academic laboratory and has begun to make it a technique of importance in the areas of industrial quality control of paints, emulsions, electroplating, thin-film technology, materials fabrication, mechanical performance of engines, corrosion, and so on.

Although this book has a strong physicochemical bias, the use of IS to investigate polarization across biological cell membranes has been pursued by many investigators since 1925. Details and discussion of the historical background of this important branch of IS are given in the books of Cole [1972] and Schanne and Ruiz-Ceretti [1978].

1.1.3 Response to a Small-Signal Stimulus in the Frequency Domain

A monochromatic signal $\nu(t) = V_m \sin(\omega t)$, involving the single-frequency $\nu \equiv \omega/2\pi$, is applied to a cell, and the resulting steady-state current $i(t) = I_m \sin(\omega t + \theta)$ measured. Here θ is the phase difference between the voltage and the current; it is zero for purely resistive behavior. The relation between system properties and response to periodic voltage or current excitation is very complex in the time domain. In general, the solution of a system of differential equations is required. Response of capacitive and inductive elements is given as $i(t) = [dv(t)/dt]C$ and $v(t) = [di(t)/dt]L$ correspondingly, and combination of many such elements can produce an intractable complex problem.

Fortunately, the use of Fourier transformation allows one to simplify significantly the mathematical treatment of this system. The aforementioned differential equations can be transformed into $I(j\ \omega) = C{\cdot}\omega{\cdot}j{\cdot}V(j\ \omega)$ and $I(j\ \omega) = V(j\ \omega)/(L{\cdot}\omega{\cdot}j)$. Here $j \equiv \sqrt{-1}$, which is also often denoted in the literature as "*i*." For the case of sine-wave excitation as aforementioned, Fourier transforms of voltage and current $V(j\,\omega)$ and $I(j\,\omega)$ become $V_{\mathrm{m}}\pi$ and $I_{\mathrm{m}}\pi{\cdot}\exp(\theta j)$, respectively. It can be easily seen that in frequency domain voltage/current relations can be rearranged to a form similar to Ohm's law for dc current: $I(j\ \omega) = V(j\ \omega)/Z(j\,\omega)$ where for capacitance the complex quantity $Z(j\,\omega)$ is $1/(C{\cdot}\omega{\cdot}j)$ and for inductance $Z(j\,\omega)$ is $L{\cdot}\omega{\cdot}j$. The complex quantity $Z(j\ \omega)$ is defined as the "impedance function," and its value at a particular frequency is "impedance" of the electric circuit. For simplicity, $Z(j\ \omega)$ is usually written as just $Z(\omega)$. Because of this Ohm's law-like relationship between complex current and voltage, the impedance of a circuit with multiple elements is calculated using the same rules as with multiple resistors, which greatly simplifies calculations.

Impedance may be defined not only for discrete systems but also for arbitrary distributed systems as the Fourier transform of the differential equation, defining the voltage response divided by the Fourier transform of the periodic current excitation: $Z(j\ \omega) = F\{v(t)\}/F\{i(t)\}$. Here the $F\{\ \}$ operator denotes a Fourier transform. However, Fourier transformation only reduces differential equations to simple Ohm's law-like form under conditions of linearity, causality, and stationarity of the system; therefore impedance is properly defined only for systems satisfying these conditions.

The concept of electrical impedance was first introduced by Oliver Heaviside in the 1880s and was soon developed in terms of vector diagrams and complex representation by A. E. Kennelly and especially C. P. Steinmetz. Impedance is a more general concept than resistance because it takes phase differences into account, and it has become a fundamental and essential concept in electrical engineering. IS is thus just a specific branch of the tree of electrical measurements. The magnitude and direction of a planar vector in a right-hand orthogonal system of axes can be expressed by the vector sum of the components a and b along the axes, that is, by the complex number $Z = a + jb$. The imaginary number $j \equiv \sqrt{-1} \equiv \exp(j\pi/2)$ indicates an anticlockwise rotation by $\pi/2$ relative to the x-axis. Thus, the real part of Z, a, is in the direction of the real axis x, and the imaginary part b is along the y-axis. An impedance $Z(\omega) = Z' + jZ''$ is such a vector quantity and may be plotted in the plane with either rectangular or polar coordinates, as shown in Figure 1.1.1. Here the two rectangular coordinate values are clearly

$$\mathrm{Re}(Z) \equiv Z' = |Z|\cos(\theta) \quad \text{and} \quad \mathrm{Im}(Z) \equiv Z'' = |Z|\sin(\theta) \tag{1}$$

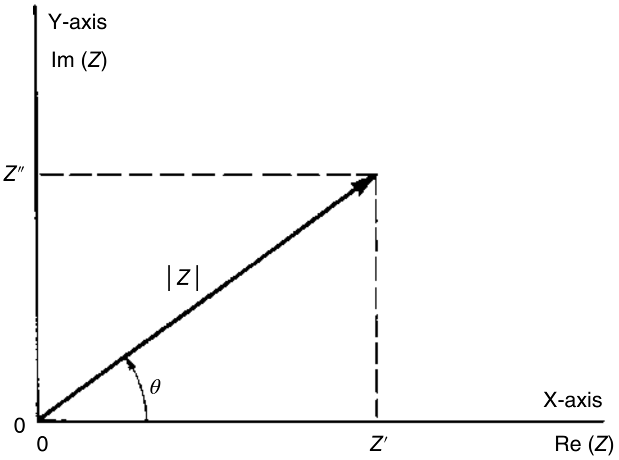

FIGURE 1.1.1 The impedance Z plotted as a planar vector using rectangular and polar coordinates.

with the phase angle

$$\theta = \tan^{-1}\left(\frac{Z''}{Z'}\right) \tag{2}$$

and the modulus

$$|Z| = \left[(Z')^2 + (Z'')^2\right]^{1/2} \tag{3}$$

This defines the Argand diagram or complex plane, widely used in both mathematics and electrical engineering. In polar form, Z may now be written as $Z(\omega) = |Z|\ \exp(j\theta)$, which may be converted to rectangular form through the use of the Euler relation $\exp(j\theta) = \cos(\theta) + j\ \sin(\theta)$. It will be noticed that the original time variations of the applied voltage and the resulting current have disappeared and the impedance is time invariant (provided the system itself is time invariant).

In general, Z is frequency dependent, as defined previously. Conventional IS consists of the (nowadays often automated) measurement of Z as a function of ν or ω over a wide frequency range. It is from the resulting structure of the $Z(\omega)$ versus ω response that one derives information about the electrical properties of the full electrode–material system.

For nonlinear systems, that is, most real electrode–material systems, IS measurements in either the time or the frequency domain are useful and meaningful in general only for signals of magnitude such that the overall electrode–material system response is electrically linear. This requires that the response to the sum of two separate input-measuring signals applied simultaneously be the sum of the responses of the signals applied separately. A corollary is that the application of a monochromatic signal, one involving $\sin(\omega t)$, results in no, or at least negligible, generation of harmonics in the output, that is, components with frequencies $n\nu$ for $n = 2, 3, \ldots$. Both solid and liquid electrochemical systems tend to show strong nonlinear behavior, especially in their interfacial response, when applied voltages or currents are large. But so long as the applied potential difference (p.d.) amplitude V_m is less than the thermal voltage, $V_\mathrm{T} \equiv RT/F \equiv kT/e$, about 25 mV at 25°C, it can be shown that the basic differential equations that govern the response of the system become linear to an excellent approximation. Here k is Boltzmann's constant, T the absolute temperature, e the proton charge, R the gas constant, and F the faraday. Thus if the applied amplitude V_m is appreciably less than V_T, the system will respond linearly. Note that in the linear regime, it is immaterial as far as the determination of $Z(\omega)$ is concerned whether a known $\nu(\omega t)$ is applied and the current measured or a known $i(\omega t)$ applied and the resulting voltage across the cell measured. When the system is nonlinear, this reciprocity no longer holds.

1.1.4 Impedance-Related Functions

The impedance has frequently been designated as the ac impedance or the complex impedance. Both these modifiers are redundant and should be omitted. Impedance without a modifier always means impedance applied in the frequency domain and usually measured with a monochromatic signal. Even when impedance values are derived by Fourier transformation from the time domain, the impedance is still defined for a set of individual frequencies and is thus an ac impedance in character.

Impedance is by definition a complex quantity and is only real when $\theta = 0$ and thus $Z(\omega) = Z'(\omega)$, that is, for purely resistive behavior. In this case the impedance is completely frequency independent. When Z' is found to be a variable function of frequency, the Kronig–Kramers (Hilbert integral transform) relations (Macdonald and Brachman [1956]), which holistically connect real and imaginary parts with each other, ensure that Z'' (and θ) cannot be zero over all frequencies but must vary with frequency as well. Thus it is only when $Z(\omega) = Z'$, independent of frequency, so $Z' = R$, an ordinary linear resistance, that $Z(\omega)$ is purely real.

There are several other measured or derived quantities related to impedance that often play important roles in IS. All of them may be generically called immittances. First is the admittance,

TABLE 1.1.1 Relations between the Four Basic Immittance Functions

	M	Z	Y	ε
M	M	μZ	μY^{-1}	ε^{-1}
Z	$\mu^{-1}M$	Z	Y^{-1}	$\mu^{-1}\varepsilon^{-1}$
Y	μM^{-1}	Z^{-1}	Y	$\mu\varepsilon$
ε	M^{-1}	$\mu^{-1}Z^{-1}$	$\mu^{-1}Y$	ε

$\mu \equiv j\omega C_c$, where C_c is the capacitance of the empty cell.

$Y \equiv Z^{-1} \equiv Y' + jY''$. In the complex domain where ν, i, and Z are all taken complex, we can write $\nu = Zi$ or alternatively $i = Y\nu$. It is also customary in IS to express Z and Y in terms of resistive and capacitance components as $Z = R_s(\omega) - jX_s(\omega)$ and $Y = G_p(\omega) + jB_p(\omega)$, where the reactance $X_s \equiv [\omega C_s(\omega)]^{-1}$ and the susceptance $B_p \equiv \omega C_p(\omega)$. Here the subscripts s and p stand for "series" and "parallel."

The other two quantities are usually defined as the modulus function $M = j\omega C_c Z = M' + jM''$ and the complex dielectric constant or dielectric permittivity $\varepsilon = M^{-1} \equiv Y/(j\omega C_c) \equiv \varepsilon' - j\varepsilon''$. In these expressions $C_c \equiv \varepsilon_0 A_c / l$ is the capacitance of the empty measuring cell of electrode area A_c and electrode separation length l. The quantity ε_0 is the dielectric permittivity of free space, 8.854×10^{-12} F/m. The dielectric constant ε is often written elsewhere as ε^* or $\hat{\varepsilon}$ to denote its complex character. Here we shall reserve the superscript asterisk to denote complex conjugation; thus $Z^* = Z' - jZ''$. The interrelations between the four immittance functions are summarized in Table 1.1.1.

The modulus function $M = \varepsilon^{-1}$ was apparently first introduced by Schrama [1957] and has been used appreciably by McCrum *et al.* [1967], Macedo *et al.* [1972b], and Hodge *et al.* [1975, 1976]. The use of the complex dielectric constant goes back much further but was particularly popularized by the work of Cole and Cole [1941], who were the first to plot ε in the complex plane.

Some authors have used the designation *modulus spectroscopy* to denote small-signal measurement of M versus ν or ω. Clearly, one could also define admittance and dielectric permittivity spectroscopy. The latter is just another way of referring to ordinary dielectric constant and loss measurements. Here we shall take the general term *IS* to include all these other very closely related approaches. Thus IS also stands for *immittance spectroscopy*. The measurement and use of the complex $\varepsilon(\omega)$ function is particularly appropriate for dielectric materials, those with very low or vanishing conductivity, but all four functions are valuable in IS, particularly because of their different dependence on and weighting with frequency.

1.1.5 Early History

IS is particularly characterized by the measurement and analysis of some or all of the four impedance-related functions Z, Y, M, and ε, and the plotting of these functions in the complex plane. Such plotting can, as we shall see, be very helpful in interpreting the small-signal AC response of the electrode–material system being investigated. Historically, the use of Z and Y in analyzing the response of electrical circuits made up of lumped (ideal) elements (R, L, and C) goes back to the beginning of the discipline of electrical engineering. An important milestone for the analysis of real systems, that is, ones distributed in space, was the plotting by Cole and Cole [1941] of ε' and ε'' for dielectric systems in the complex plane, now known as a Cole–Cole plot, an adaption at the dielectric constant level of the circle diagram of electrical engineering (Carter [1925]), exemplified by the Smith–Chart impedance diagram (Smith [1939, 1944]). Further, Z and Y have been widely used in theoretical treatments of semiconductor and ionic systems and devices since at least 1947 (see, e.g., Randles [1947], Jaffé [1952], Chang and Jaffé [1952], Macdonald [1953a], and Friauf [1954]). Complex plane plots have sometimes been called Nyquist diagrams. This is a misnomer, however, since Nyquist diagrams refer to transfer function (three- or four-terminal) response, while conventional complex plane plots involve only two-terminal input immittances.

On the experimental side, one should mention the early work of Randles and Somerton [1952] on fast reactions in supported electrolytes; no complex plane plotting appeared here. But complex plane plotting of G_p/ω versus C_p was used by Macdonald [1955] for experimental results on photoconducting alkali halide single crystals. Apparently the first plotting of impedance in the impedance plane for aqueous electrolytes was that of Sluyters [1960] (theory) and Sluyters and Oomen [1960] (experiment). The use of admittance plane plotting for accurate conductivity determination of solid electrolytes was introduced by Bauerle [1969], the first important paper to deal with IS for ionic solids directly. Since then, there have been many pertinent theoretical and experimental papers dealing with IS and complex plane plots. Many of them will be cited later, and we conclude this short survey of early history pertinent to IS with the mention of three valuable reviews: Sluyters-Rehbach and Sluyters [1970], Armstrong *et al.* [1978], and Archer and Armstrong [1980]. The first and second of these deal almost entirely with liquid electrolytes but are nevertheless somewhat pertinent to IS for solids.

1.2 ADVANTAGES AND LIMITATIONS

Although we believe that the importance of IS is demonstrated throughout this monograph by its usefulness in the various applications discussed, it is of some value to summarize the matter briefly here. IS is becoming a popular analytical tool in materials research and development because it involves a relatively simple electrical measurement that can readily be automated and whose results may often be correlated with many complex materials variables: from mass transport, rates of chemical reactions, corrosion, and dielectric properties, to defects, microstructure, and compositional influences on the conductance of solids. IS can predict aspects of the performance of chemical sensors and fuel cells, and it has been used extensively to investigate membrane behavior in living cells. It is useful as an empirical quality control procedure, yet it can contribute to the interpretation of fundamental electrochemical and electronic processes.

A flow diagram of a general characterization procedure using IS is presented in Figure 1.2.1. Here CNLS stands for complex nonlinear least squares fitting (see Section 3.2.2). Experimentally obtained impedance data for a given electrode–materials system may be analyzed by using an exact mathematical model based on a plausible physical theory that predicts theoretical impedance $Z_t(\omega)$ or by a relatively empirical equivalent circuit whose impedance predictions may be denoted by $Z_{ec}(\omega)$. In case either of the relatively empirical equivalent circuit or of the exact mathematical model, the parameters can be estimated and the experimental $Z_e(\omega)$ data compared with either the predicted equivalent circuit impedance $Z_{ec}(\omega)$ or the theoretical impedance $Z_t(\omega)$. Such fitting is most accurately accomplished by the CNLS method described and illustrated in Section 3.2.2.

An analysis of the charge transport processes likely to be present in an experimental cell (the physical model) will often suggest an equivalent circuit of ideal resistors and capacitors (even inductors or negative capacitors in some instances) and may account adequately for the observed IS response. For example, Schouler *et al.* [1983] found that the effects of densification by sintering a polycrystalline electrolyte will reduce the magnitude of the resistance across the grain boundaries and simultaneously decrease the surface area associated with the interface capacitance. These components will clearly be electrically in parallel in this situation. Their combination will be in series with other similar subcircuits representing such processes as the ionization of oxygen at the electrodes.

In another example, the oxidation–reduction reaction for the Zn^{2+} couple in an aqueous solution with a dropping mercury electrode (Sluyters and Oomen [1960]) can be represented by a reaction resistance R_R, arising from the transfer of electrons between the electrode and the solution, in parallel with a capacitor C_R associated with the space-charge diffuse double layer near the electrode surface. It is not difficult to calculate the theoretical impedance for such a circuit in terms of the parameters R_R and C_R. From an analysis of the parameter values in a plausible equivalent circuit as the experimental conditions are changed, the materials system can be characterized by analysis of its observed impedance response, leading to estimates of its microscopic parameters such as charge mobilities, concentrations, and electron transfer reaction rates.

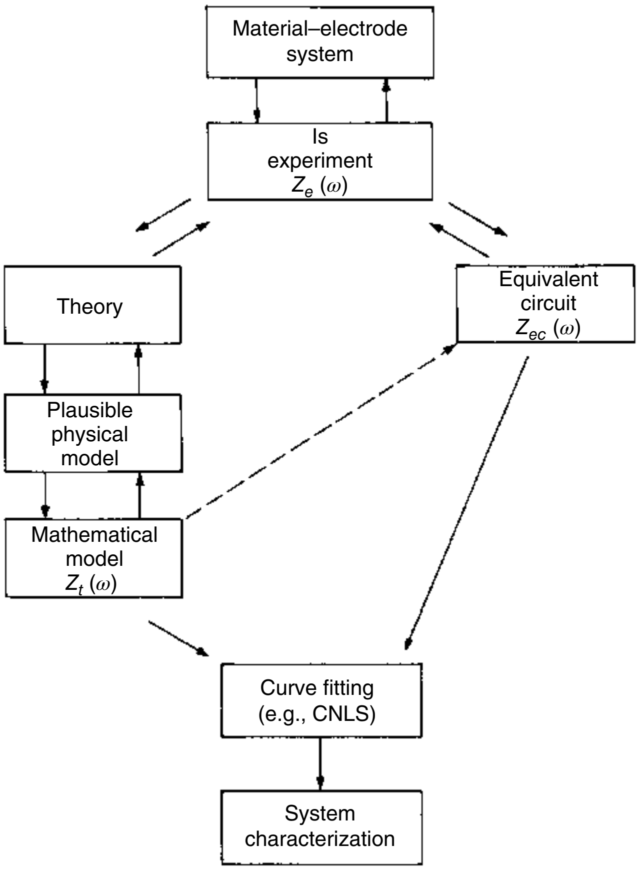

FIGURE 1.2.1 Flow diagram for the measurement and characterization of a material–electrode system.

The disadvantages of IS are primarily associated with possible ambiguities in interpretation. An important complication of analyses based on an equivalent circuit (e.g., Bauerle [1969]) is that ordinary ideal circuit elements represent ideal lumped-constant properties. Inevitably, all electrolytic cells are distributed in space, and their microscopic properties may be also independently distributed. Under these conditions, ideal circuit elements may be inadequate to describe the electrical response. Thus, it is often found that $Z_e(\omega)$ cannot be well approximated by the impedance of an equivalent circuit involving only a finite number of ordinary lumped-constant elements. It has been observed by many in the field that the use of distributed impedance elements (e.g., constant-phase elements (CPEs) (see Section 2.2.2.2)) in the equivalent circuit greatly aids the process of fitting observed impedance data for a cell with distributed properties.

There is a further serious potential problem with equivalent circuit analysis, not shared by the direct comparison with $Z_t(\omega)$ of a theoretical model: what specific equivalent circuit out of an infinity of possibilities should be used if one is necessary? An equivalent circuit involving three or more circuit elements can often be rearranged in various ways and still yield exactly the same $Z_{ec}(\omega)$. For the different interconnections, the values of the elements will have to be different to yield the same $Z_{ec}(\omega)$ for all ω, but an essential ambiguity is present. An example is presented in Figure 1.2.2. In these circuits the impedance Z_i is arbitrary and may be made up of either lumped elements, distributed elements, or a combination of these types. Examples of other circuits that demonstrate this type of ambiguity will be presented in Section 2.2.2.3. Which one of two or more circuits that all yield exactly the same $Z_{ec}(\omega)$ for all ω should be used for physicochemical analysis and interpretation? This question cannot be answered for a single set of $Z_e(\omega)$ data alone. An approach to its solution can only be made by employing

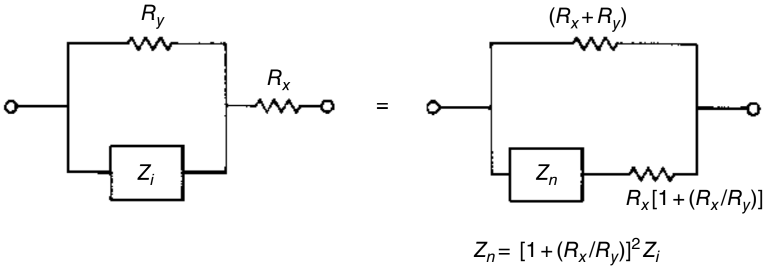

FIGURE 1.2.2 An example of different circuits with the same overall impedance at all frequencies.

physical intuition and by carrying out several $Z_e(\omega)$ sets of measurements with different conditions, as discussed in Section 2.2.2.3.

1.2.1 Differences between Solid-State and Aqueous Electrochemistry

The electrochemist who works with aqueous electrolytes has available to him/her at least one major stratagem not accessible to those who work with solid electrolytes. If he/she is interested in the interfacial behavior of a particular charged species, he/she is usually free to add to the solution an excess of a second electrolyte, the ions of which are neither adsorbed nor react at the interface but which by sheer numbers are able to screen the interior of the electrolyte from any electric field and cause nearly all the potential drop to occur within a few angstroms of the interface. The investigator is thus (at least by assumption) freed from having to take into account the effect of a nonuniform electric field on the transport of the electroactive species through the bulk electrolyte and need not (again by assumption) puzzle over the fraction of the applied signal that directly governs the exchange of ions or electrons between the electrode surface and the adjacent layer of electrolyte. The added electrolyte species that thus simplifies the interpretation of the experimental results is termed the *indifferent* or *supporting electrolyte*, and systems thus prepared are termed *supported systems*. Solid electrolytes must necessarily be treated as unsupported systems, even though they may display some electrical characteristics usually associated with supported ones. The distinction between unsupported and supported situations is a crucial one for the interpretation of IS results.

It is thus unfortunate that there has been a tendency among some workers in the solid electrolyte field to take over many of the relatively simple theoretical results derived for supported conditions and use them uncritically in unsupported situations, where the supported models and formulas rarely apply adequately. For example, the expression for the Warburg impedance for a redox reaction in a supported situation is often employed in the analysis of data on unsupported situations where the parameters involved are quite different (see, e.g., Sections 2.2.3.2 and 2.2.3.3).

There are a few other important distinctions between solid and liquid electrolytes. While liquid electrolytes and many solid electrolytes have negligible electronic conductivity, quite a number of solid electrolytes can exhibit substantial electronic conductivity, especially for small deviations from strict stoichiometric composition. Solid electrolytes may be amorphous, polycrystalline, or single crystal, and charges of one sign may be essentially immobile (except possibly for high temperatures and over long time spans). On the other hand, all dissociated charges in a liquid electrolyte or fused salt are mobile, although the ratio between the mobilities of positive and negative charges may differ appreciably from unity. Further, in solid electrolytes, mobile ions are considered to be able to move as close to an electrode as permitted by ion-size steric considerations. But in liquid electrolytes, a compact inner or Stern layer composed of solvent molecules, for example, H_2O, immediately next to the electrode, is usually present. This layer may often be entirely devoid of ions and only has some in it when the ions are specifically adsorbed at the electrode or react there. Thus capacitative effects in electrode interface regions can be considerably different between solid and liquid electrolyte systems.

1.3 ELEMENTARY ANALYSIS OF IMPEDANCE SPECTRA

1.3.1 Physical Models for Equivalent Circuit Elements

A detailed physicoelectrical model of all the processes that might occur in investigations on an electrode–material system may be unavailable, premature, or perhaps too complicated to warrant its initial use. One then tries to show that the experimental impedance data $Z_e(\omega)$ may be well approximated by the impedance $Z_{ec}(\omega)$ of an equivalent circuit made up of ideal resistors, capacitors, perhaps inductances, and possibly various distributed circuit elements. In such a circuit a resistance represents a conductive path, and a given resistor in the circuit might account for the bulk conductivity of the material or even the chemical step associated with an electrode reaction (see, e.g., Randles [1947] or Armstrong *et al.* [1978]). Similarly, capacitances and inductances will be generally associated with space-charge polarization regions and with specific adsorption and electrocrystallization processes at an electrode. It should be pointed out that ordinary circuit elements, such as resistors and capacitors, are always considered as lumped-constant quantities that involve ideal properties. But all real resistors are of finite size and are thus disturbed in space; they therefore always involve some inductance, capacitance, and time delay of response as well as resistance. These residual properties are unimportant over wide frequency ranges and therefore usually allow a physical resistor to be well approximated in an equivalent circuit by an ideal resistance, one which exhibits only resistance over all frequencies and yields an immediate rather than a delayed response to an electrical stimulus.

The physical interpretation of the distributed elements in an equivalent circuit is somewhat more elusive. They are, however, essential in understanding and interpreting most impedance spectra. There are two types of distributions with which we need to be concerned. Both are related, but in different ways, to the finite spatial extension of any real system. The first is associated directly with nonlocal processes, such as diffusion, which can occur even in a completely homogeneous material, one whose physical properties, such as charge mobilities, are the same everywhere. The other type, exemplified by the CPE, arises because microscopic material properties are themselves often distributed. For example, the solid electrode–solid electrolyte interface on the microscopic level is not the often presumed smooth and uniform surface. It contains a large number of surface defects such as kinks, jags, and ledges, local charge inhomogeneities, two- and three-phase regions, adsorbed species, and variations in composition and stoichiometry. Reaction resistance and capacitance contributions differ with electrode position and vary over a certain range around a mean, but only their average effects over the entire electrode surface can be observed. The macroscopic impedance that depends, for example, on the reaction rate distribution across such an interface is measured as an average over the entire electrode. We account for such averaging in our usual one-dimensional treatments (with the dimension of interest perpendicular to the electrodes) by assuming that pertinent material properties are continuously distributed over a given range from minimum to maximum values. For example, when a given time constant, associated with an interface or bulk processes, is thermally activated with a distribution of activation energies, one passes from a simple ideal resistor and capacitor in parallel or series to a distributed impedance element, for example, the CPE, which exhibits more complicated frequency response than a simple undistributed RC time constant process (Macdonald [1984, 1985a, c, d], McCann and Badwal [1982]).

Similar property distributions occur throughout the frequency spectrum. The classical example for dielectric liquids at high frequencies is the bulk relaxation of dipoles present in a pseudoviscous liquid. Such behavior was represented by Cole and Cole [1941] by a modification of the Debye expression for the complex dielectric constant and was the first distribution involving the important CPE, defined in Section 2.1.2.3. In normalized form the complex dielectric constant for the Cole–Cole distribution may be written as

$$\frac{\varepsilon-\varepsilon_\infty}{\varepsilon_s-\varepsilon_\infty}=\left[1+(j\omega\tau_0)^{1-\alpha}\right]^{-1} \tag{1}$$

where ε is the dielectric constant, ε_s and ε_∞ the static and high-frequency-limiting dielectric constants, τ_0 the mean relaxation time, and α a parameter describing the width of the material property distribution (in this case a distribution of dielectric relaxation times in frequency space).

1.3.2 Simple RC Circuits

Figure 1.3.1 shows two RC circuits common in IS and typical Z and Y complex plane responses for them. The response of Figure 1.3.1a is often present (if not always measured) in IS results for solids and liquids. Any electrode–material system in a measuring cell has a geometrical capacitance $C_g \equiv C_\infty = C_1$ and a bulk resistance $R_b \equiv R_\infty = R_1$ parallel with it. These elements lead to the time constant $\tau_D = R_\infty C_\infty$, the dielectric relaxation time of the basic material. Usually, τ_D is the smallest time constant of interest in IS experiments. It is often so small ($<10^{-7}$ s) that for the highest angular frequency applied, $\omega_{\max}$, the condition $\omega_{\max}\tau_D \ll 1$ is satisfied and little or nothing of the impedance plane curve of Figure 1.3.1b is seen. It should be noted, however, that lowering the temperature will often increase τ_D and bring the bulk arc within the range of measurement. Since the peak frequency of the complete semicircle in Figure 1.3.1b, ω_p, satisfies $\omega_p\tau_D = 1$, it is only when $\omega_{\max}\tau_D \gg 1$ that nearly the full curve in Figure 1.3.1b is obtained. Although the bulk resistance is often not appreciably distributed, particularly for single crystals, when it is actually distributed, the response of the circuit often leads to a partial semicircle in the Z plane, one whose center lies below the real axis, instead of a full semicircle with its center on the real axis. Since this distributed-element situation is frequently found for processes in the $\omega \ll \tau_D^{-1}$ frequency range, however, we shall examine in detail one simple representation of it shortly.

Besides $R_1 = R_\infty$ and $C_1 = C_\infty$, one often finds parallel R_1, C_1 response associated with a heterogeneous electrode reaction. For such a case we would set $R_1 = R_R$ and $C_1 = C_R$, where R_R is a reaction

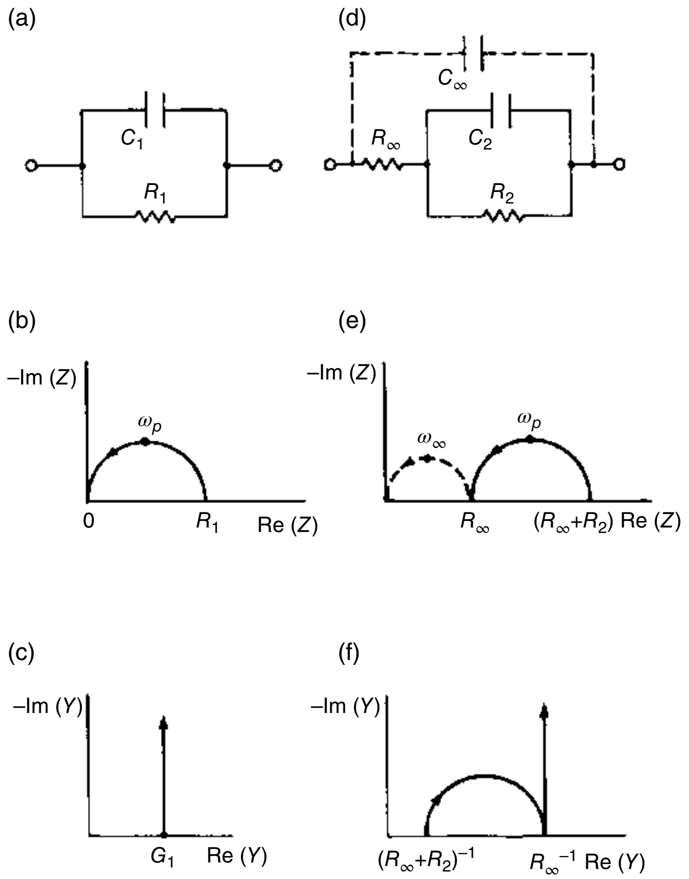

FIGURE 1.3.1 (a) and (d) show two common RC circuits, (b) and (e) show their impedance plane plots, and (c) and (f) show their admittance plane plots. Arrows indicate the direction of increasing frequency.

resistance and C_R is the diffuse double-layer capacitance of the polarization region near the electrode in simplest cases. The circuit of Figure 1.3.1d combines the aforementioned possibilities when $R_2 = R_R$ and $C_2 = C_R$. The results shown in Figure 1.3.1e and f are appropriate for the well-separated time constants, $R_\infty R_\infty \ll R_2C_2$. It is also possible that a parallel RC combination can result from specific adsorption at an electrode, possibly associated with delayed reaction processes. The response arising from R_∞ and C_∞ in Figure 1.3.1e is shown dotted to remind one that it often occurs in too high a frequency region to be easily observed. Incidentally, we shall always assume that the capacitance and resistance of leads to the measuring cell have been subtracted out (e.g., by using the results of a preliminary calibration of the system with the cell empty or shorted) so that we always deal only with the response of the material–electrode system alone.

In the complex plane plots, the arrows show the direction of increasing frequency. Further, $G_1 \equiv R_1^{-1}$, $G_\infty \equiv R_\infty^{-1}$, $G_2 \equiv R_2^{-1}$. Because IS results usually involve capacitance and rarely involve inductance, it has become customary to plot impedance in the –Im(Z), Re(Z) plane rather than the Im(Z), Re(Z) plane, thereby ensuring that the vast majority of all curves fall in the first quadrant, as in Figure 1.3.1b. This procedure is also equivalent to plotting $Z^* = Z' - iZ''$ rather than Z, so we can alternatively label the ordinate Im(Z^*) instead of –Im(Z). Both choices will be used in the rest of this work.

The admittance of the parallel RC circuit of Figure 1.3.1a is just the sum of the admittances of the two elements, that is,

$$Y_a = G_1 + j\omega C_1 \tag{2}$$

It immediately follows that

$$Z_a = Y_a^{-1} = \frac{R_1}{R_1 Y_a} = \frac{R_1}{1 + j\omega R_1 C_1} \tag{3}$$

This result can be rationalized by multiplying $[1 - j\omega R_1C_1]$, the complex conjugate of $[1 + j\omega R_1C_1]$, to both numerator and denominator. The response of the Figure 1.3.1a circuit is particularly simple when it is plotted in the Y plane, as in Figure 1.3.1c. To obtain the overall admittance of the Figure 1.3.1d circuit, it is simplest to add R_∞ to the expression for Z_a previously mentioned with $R_1 \to R_2$ and $C_1 \to C_2$, convert the result to an admittance by inversion, and then add the $j\omega C_\infty$ admittance. The result is

$$Y_d = j\omega C_\infty + \frac{1 + j\omega R_2 C_2}{(R_2 + R_\infty) + j\omega C_2 R_2 R_\infty}. \tag{4}$$

Although complex plane data plots, such as those in Figure 1.3.1b, c, e, and f in which frequency is an implicit variable, can show response patterns that are often very useful in identifying the physicochemical processes involved in the electrical response of the electrode–material system, the absence of explicit frequency-dependent information is frequently a considerable drawback. Even when frequency values are shown explicitly in such two-dimensional (2D) plots, it is usually found that with either equal intervals in frequency or equal frequency ratios, the frequency points fall very nonlinearly along the curves. The availability of computerized plotting procedures makes the plotting of all relevant information in a single graph relatively simple. For example, three-dimensional (3D) perspective plotting, as introduced by Macdonald *et al*. [1981], displays the frequency dependence along a new log (v) axis perpendicular to the complex plane (see Section 3.2). For multi-time-constant response in particular, this method is particularly appropriate. The full response information can alternately be plotted with orthographic rather than perspective viewing.

1.3.3 Analysis of Single Impedance Arcs

Analysis of experimental data that yield a full semicircular arc in the complex plane, such as that in Figure 1.3.1b, can provide estimates of the parameters R_1 and C_1 and hence lead to quantitative estimates of conductivity, faradic reaction rates, relaxation times, and interfacial capacitance (see detailed discussion in Section 2.2.3.3). In practice, however, experimental data are only rarely found to yield a full semicircle with its center on the real axis of the complex plane. There are three common perturbations that may still lead to at least part of a semicircular arc in the complex plane:

1. The arc does not pass through the origin, either because there are other arcs appearing at higher frequencies or because $R_\infty > 0$.
2. The center of an experimental arc is frequently displaced below the real axis because of the presence of distributed elements in the material–electrode system. Similar displacements may also be observed in any of the other complex planes plots (Y, M, or $\in$). The relaxation time τ is then not single-valued but is distributed continuously or discretely around a mean, $\tau_m = \omega_m^{-1}$. The angle θ by which such a semicircular arc is depressed below the real axis is related to the width of the relaxation time distribution and as such is an important parameter.
3. Arcs can be substantially distorted by other relaxations whose mean time constants are within two orders of magnitude or less of that for the arc under consideration. Many of the spectra shown in following chapters involve overlapping arcs.

We shall begin by considering simple approximate analysis methods of data yielding a single, possibly depressed, arc. Suppose that IS data plotted in the impedance plane (actually the Z^* plane) show typical depressed circular arc behavior, such as that depicted in Figure 1.3.2. Here we have included R_∞ but shall initially ignore any effect of C_∞. We have defined some new quantities in this figure that will be used in the analysis to yield estimates of the parameters R_∞, $R_R \equiv R_0 - R_\infty$, τ_R, and the fractional exponent ψ_{ZC}, parameters that fully characterize the data when they are well represented by the distributed-element ZARC impedance expression (see Section 2.2.2.2):

$$Z - R_\infty \equiv Z_{ZARC} \equiv (R_0 - R_\infty) I_Z \tag{5}$$

where

$$IZ \equiv [1 + (j\omega\tau_R)^{\psi_{ZC}}]^{-1} \equiv [1 + (js)^{\psi_{ZC}}]^{-1} \tag{6}$$

Here $s \equiv \omega\tau_R$ is a normalized frequency variable and I_Z is the normalized, dimensionless form of Z_{ZARC}. Notice that it is exactly the same as the similarly normalized Cole–Cole dielectric response

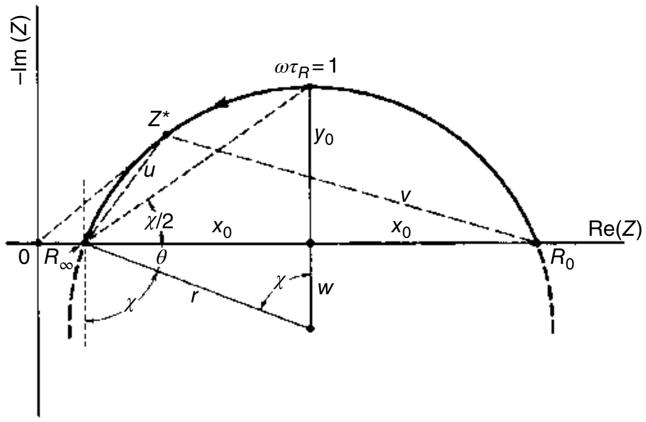

FIGURE 1.3.2 Impedance plane plot for a depressed circular arc showing definitions of quantities used in its analysis.

function of Eq. (1) when we set $\psi_{ZC} = 1-\alpha$. We can also alternatively write the ZARC impedance as the combination of the resistance R_R in parallel with the CPE impedance Z_{CPE} (see Section 2.2.2.2). The CPE admittance is (Macdonald [1984])

$$Y_{CPE} = Z_{CPE}^{-1} \equiv A_0(j\omega)^{\psi_{ZC}} \equiv (j\omega\tau_R)^{\psi_{ZC}} \tag{7}$$

Then Eq. (5) may be expressed as

$$Z_{ZARC} = \frac{R_R}{1+B_0(j\omega)^{\psi_{ZC}}}, \tag{8}$$

where $B_0 \equiv \tau_R^{\psi_{ZC}} \equiv R_R A_0$. The fractional exponent ψ_{ZC} satisfies $0 \le \psi_{ZC} \le 1$.

Let us start by considering two easy-to-use approximate methods of estimating the parameters, methods often adequate for initial approximate characterization of the response. The estimates obtained by these approaches may also be used as initial values for the more complicated and much more accurate CNLS method described and illustrated in Section 3.2.2. Note that the single $R_R C_R$ situation, where $\theta = 0$ and $\psi_{ZC} = 1$, is included in the analysis described in the succeeding text.

From the Figure 1.3.2, $-Z''$ reaches its maximum value, y_0, when $\omega = \omega_m = \tau_R^{-1}$ and thus $s = 1$. At this point the half-width of the arc on the real axis is $Z' - R_\infty = x_0 \equiv R_R/2$. Now from the data, the complex plane plot, and estimated values of x_0, y_0, and ω_m, one can immediately obtain estimates of R_∞, R_0, R_R, and τ_R. In order to obtain θ, one must, of course, find the direction of the circle center. The easiest graphical method is to draw on the Z^* plane plot several lines perpendicular to the semicircle; the center will be defined by their intersection. Two other more accurate approaches will be described in the succeeding text. Incidentally, when there is more than one arc present and there is some overlap that distorts the right, lower-frequency side of the arc, the present methods can still be used without appreciable loss of accuracy, provided overlap distortion is only significant for $\omega < \omega_m$, that is, on the right side of the center of the left arc. Then all parameters should be estimated from the left side of the arc, that is, for $\omega \ge \omega_m$. A similar approach may be used when data are available only for $\omega \le \omega_m$. From Figure 1.3.2 and Eq. (5), we readily find that $\theta = \pi/2 - x \equiv (\pi/2)(1-\psi_{ZC})$; thus when $\psi_{ZC} = 1$ there is no depression and one has simple single-time-constant ($\tau_R \equiv R_R C_R$) Debye response with $A_0 \equiv C_R$. When $\psi_{ZC} < 1$, $\tau_R = (R_R A_0)^{1/\psi_{ZC}}$, but an ideal C_R capacitor cannot be directly defined, reflecting the distributed nature of the response.

The rest of the analysis proceeds as follows. First, one may obtain an estimate of ψ_{ZC} from the θ value using $\psi_{ZC} = 1 - 2\theta/\pi$. But a superior alternative to first obtaining θ by finding the circle center approximately is to use the values of x_0 and y_0 defined on the Figure 1.3.2. For simplicity, it will be convenient to define

$$q \equiv (\omega\tau_R)^{\psi_{ZC}} \equiv (s)^{\psi_{ZC}} \tag{9}$$

$$\chi \equiv \frac{\pi}{2} - \theta \equiv \frac{\pi}{2}\psi_{ZC} \tag{10}$$

and note that

$$x_0 \equiv \frac{R_0 - R_\infty}{2} \equiv \frac{R_R}{2} \tag{11}$$

We may now rewrite Eq. (6) for I_Z as

$$I_Z(q,\chi) = \frac{[1+q\cos(\chi)] - jq\sin(\chi)}{1+2q\cos(\chi)+q^2} \tag{12}$$

For $q = 1$, the peak point, one finds

$$I_Z(1,\chi) = 0.5\left[1 - j\tan\left(\frac{\chi}{2}\right)\right] \tag{13}$$

Let us further define for later use the quantity

$$\psi_{\mathrm{J}} \equiv \tan\left(\frac{\chi}{2}\right) = \tan\left(\frac{\pi\psi_{\mathrm{ZC}}}{4}\right) \tag{14}$$

Now in general from Eq. (12), we may write

$$-\frac{I''_{\mathrm{Z}}}{I'_{\mathrm{Z}}} = \frac{q\sin(\chi)}{1+q\cos(\chi)} \tag{15}$$

which becomes, for $q = 1$,

$$\left.\frac{-I''_{\mathrm{Z}}}{I'_{\mathrm{Z}}}\right|_{q=1} = \frac{y_0}{x_0} = \tan\left(\frac{\chi}{2}\right) \equiv \psi_{\mathrm{J}} \tag{16}$$

Thus from knowledge of y_0 and x_0, one can immediately calculate χ, ψ_{J}, ψ_{ZC}, and θ. For completeness, it is worth giving expressions for w are r that follow from the Figure 1.3.2. One finds

$$w = x_0\,\mathrm{ctn}\,(\chi) = x_0\,\tan\,(\theta) = x_0\frac{1-\psi_{\mathrm{J}}^2}{2\psi_{\mathrm{J}}} \tag{17}$$

and

$$r - y_0 + w = x_0\,\csc\,(\chi) = x_0\,\sec\,(\theta) = x_0\frac{1+\psi_{\mathrm{J}}^2}{2\psi_{\mathrm{J}}} \tag{18}$$

Another method of obtaining ψ_{ZC} and θ is to first estimate R_∞ and plot $(Z-R_\infty)^{-1}$ in the Y plane. Then a spur inclined at the angle $[(\pi/2)-\theta] = \chi$ will appear whose $\omega \to 0$ intercept is $(R_0 - R_\infty)^{-1}$. A good estimate of ψ_{ZC} may be obtained from the χ value when the spur is indeed a straight line. Now at $\omega = \omega_{\mathrm{m}}$, it turns out that $B_0\omega_{\mathrm{m}}^{\psi_{\mathrm{ZC}}} = 1$. Thus one may obtain an estimate of B_0 from $\omega_{\mathrm{m}}^{-\psi_{\mathrm{ZC}}}$. Then $\tau_{\mathrm{R}} = \mathrm{B}_0^{1/\psi_{\mathrm{ZC}}} = \omega_{\mathrm{m}}^{-1}$ and $A_0 = R_{\mathrm{R}}^{-1}B_0$. Thus all the parameters of interest have then been estimated.

The aforementioned simple methods of estimating ψ_{ZC} depend only on the determination of x_0 and y_0 from the impedance complex plane arc or on the use of a few points in the admittance plane. Although they are often adequate for initial investigation, it is worth mentioning a relatively simple alternative procedure that can be used to test the appropriateness of Eqs. (5) and (6) and obtain the parameter estimates of interest. Consider the point Z^* on the arc of Figure 1.3.2, a point marking a specific value of Z. It follows from this figure and Eq. (5) that $Z^* - R_\infty = (R_0 - R_\infty)I_{\mathrm{Z}}^* \equiv u$ and $R_0 - Z^* = (R_0 - R_\infty)\left(1 - I_{\mathrm{Z}}^*\right) \equiv v$. Therefore,

$$\ln\left|\frac{v}{u}\right| = \ln\left|\left(I_{\mathrm{Z}}^*\right)^{-1} - 1\right| = \ln(q) = \psi_{\mathrm{ZC}}[\ln(\omega) + \ln(\tau_{\mathrm{R}})] \tag{19}$$

If one assumes that R_0 and R_∞ may be determined adequately from the complex plane plot—not always a valid assumption—then v and u may be calculated from experimental Z data for a variety of frequencies. A plot of $\ln|v/u|$ versus $\ln(\omega)$ will yield a straight line with a slope of ψ_{ZC} and an intercept of $\psi_{\mathrm{ZC}}\ln(\tau_{\mathrm{R}})$, provided Eq. (19) holds. Ordinary linear least squares fitting may then be used to obtain estimates of ψ_{ZC} and $\ln(\tau_{\mathrm{R}})$.

Although a more complicated nonlinear least squares procedure has been described by Tsai and Whitmore [1982], which allows analysis of two arcs with some overlap, approximate analysis of two or more arcs without much overlap does not require this approach, and CNLS fitting is more appropriate for one or more arcs with or without appreciable overlap when accurate results are needed. In this section we have discussed some simple methods of obtaining approximate estimates of some equivalent circuit parameters, particularly those related to the common symmetrical depressed arc, the ZARC. An important aspect of material–electrode characterization is the identification of derived parameters with specific physicochemical processes in the system. This matter is discussed in detail in Sections 2.2 and 3.2 and will not be repeated here. Until such identification has been made, however, one cannot relate the parameter estimates, such as R_R, C_R, and ψ_{ZC}, to specific microscopic quantities of interest such as mobilities, reaction rates, and activation energies. It is this final step, however, yielding estimates of parameters immediately involved in the elemental processes occurring in the electrode–material system, which is the heart of characterization and an important part of IS.

1.4 SELECTED APPLICATIONS OF IS

In this section two applications will be presented, illustrating the power of the IS technique when it is applied to two very diverse areas, aqueous electrochemistry and fast ion transport in solids. These particular examples were chosen because of their historical importance and because the analysis in each case is particularly simple. Additional techniques and applications of IS to more complicated systems will be presented in Chapter 4 as well as throughout the text.

The first experimental use of complex plane analysis in aqueous electrochemistry was performed in 1960 (Sluyters and Oomen [1960]). This study is a classic illustration of the ability of IS to establish kinetic parameters in an aqueous electrochemical system. Using a standard hanging mercury drop cell, the impedance response of the $Zn(Hg)/Zn^{2+}$ couple in a 1 M $NaClO_4$ + 10^{-3} M $HClO_4$ electrolyte was examined at 298 K. For this couple, the reaction rate is such that in the frequency range of 20 Hz to 20 kHz, the kinetics of charge transfer is slower than ion diffusion in the electrolyte. The results (Figure 1.4.1) show a single semicircle characteristic of kinetic control by an electrochemical charge transfer step at the electrode–electrolyte interface. The physical model appropriate to this system is the same as that presented in Figure 1.3.1d. The semicircle beginning at the origin in Figure 1.3.1e is not observed in Figure 1.4.1 because the frequency range was limited to below 20 kHz. Thus, in Figure 1.4.1, R_∞ is the solution resistance, R_2 is the charge transfer resistance, and C_2 is the double-layer capacitance.

By solving the standard current–potential equation for an electrochemical reaction (see, e.g., Bard and Faulkner [1980]) under the conditions of kinetic control (i.e., the rate of charge transfer is much

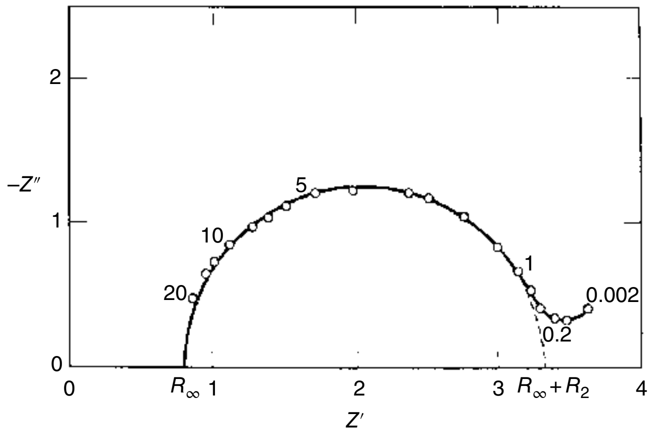

FIGURE 1.4.1 The impedance results of a $Zn(Hg)/Zn^{2+}$ couple in 1 M $NaClO_4$ + 10^{-3}N $HClO_4$ with $C_{Zn} = 8 \times 10^{-6}$ coles/cm^3 and $C_{Zn^{2+}} = 8 \times 10^{-6}$. The numbers represent the frequency in kilohertz; the axes are in arbitrary scale units. *Source:* Sluyters 1960. Reproduced with permission of John Wiley & Sons, Inc.

slower than diffusive processes in the system), the value of R_2 can be evaluated. For a known concentration of Zn at the amalgam–electrolyte interface, $C_{Zn(Hg)}$, and a known concentration of Zn^{2+} at the electrolyte–electrode interface, $C_{Zn^{2+}}$, the value of R_2 is given by Eq. (1):

$$R_2 = \frac{RT}{n^2 F^2 k (C_{Zn^{2+}})^{\alpha} \left(C_{Zn(Hg)}\right)^{1-\alpha}} \tag{1}$$

where n is the number of electrons transferred, F is Faraday's constant, k is the rate constant for the electrochemical charge transfer reaction, α is the electrochemical transfer coefficient, R is the ideal gas constant, and T is the absolute temperature. When the concentration of Zn in the amalgam is equal to the concentration of Zn ions in the solution, then the rate constant k can be determined. Results at several different equal concentrations of Zn and Zn^{2+} (Table 1.4.1) gave a mean value of $k = 3.26 \times 10^3$ cm/s. By using different concentrations of Zn and Zn^{2+}, the transfer coefficient α (Tables 1.4.2 and 1.4.3)

TABLE 1.4.1 Calculation of Rate Constant of Zn(Hg)/Zn^{2+} Couple

$C_{Zn} = C_{zn^{2+}}$ (mol/cm^3)	R_2 (Ω-cm^2)	$R_2 \times C_{Zn}$ (mol-Ω/cm)	k (cm/s)[a]
2×10^{-6}	10.17	20.3×10^{-6}	
4	4.95	19.8	
5	4.26	21.3	
8	2.41	19.3	$3.26 \times 10^{-3} \pm 3.6\%$
10	2.13	21.3	
16	1.27	20.3	
16	1.28	20.5	

[a] Calculated from the average value of $R_2 \times C_{Zn} = 20.4 \times 10^{-6}$ by $k = (R_2 C_{Zn} n^2 F^2)^{-1} RT$ according to Eq. (1).
Source: Sluyters and Oomen [1960].

TABLE 1.4.2 Calculation of Transfer Coefficient α of Zn(Hg)/Zn^{2+} Couple

C_{Zn} (mol/cm^3)	$C_{Zn^{2+}}$ (mol/cm^3)	R_2 (Ω-cm^2)	log R_2	−log $C_{Zn^{2+}}$	α[a]
16×16^{-6}	16×10^{-6}	1.28	0.107	4.796	
16	8	2.00	0.301	5.097	0.70
16	4	3.29	0.517	5.398	
16	2	5.37	0.730	5.699	

[a] From slope of −log $C_{Zn^{2+}}$ versus log R_2 plot.
Source: Sluyters and Oomen [1960].

TABLE 1.4.3 Calculation of Transfer Coefficient $1 - \alpha$ of Zn(Hg)/Zn^{2+} Couple

$C_{Zn^{2+}}$ (mol/cm^3)	C_{Zn} (mol/cm^3)	R_2 (Ω-cm^2)	log R_2	−log C_{Zn}	$1 - \alpha$[a]
16×10^{-6}	16×10^{-6}	1.28	0.107	4.796	
16×10^{-6}	8	1.56	0.193	5.097	0.29
16×10^{-6}	4	1.93	0.286	5.398	

[a] From slope of −log C_{Zn} versus log R_2 plot.
Source: Sluyters and Oomen [1960].

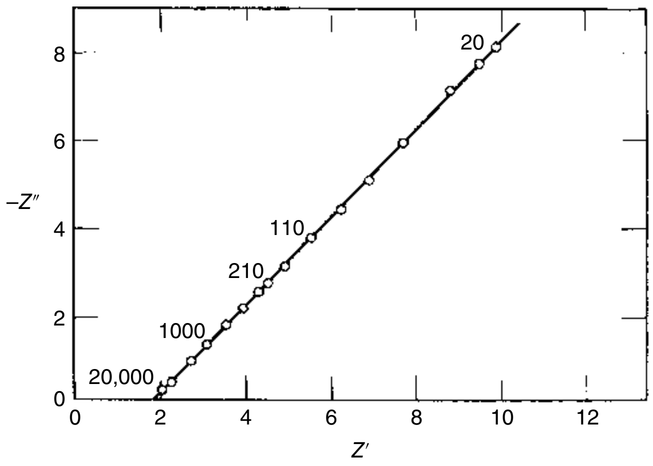

FIGURE 1.4.2 The impedance results of a Hg_2^{2+}/Hg couple in 1 M $HClO_4$ electrolyte with $C_{Hg^{2+}} = 2 \times 10^{-6}$ mol/cm^3. The numbers represent the frequency in kilohertz; the axes are in arbitrary scale units. *Source:* Sluyters 1960. Reproduced with permission of John Wiley & Sons, Inc.

was found to be 0.70. In addition, the value of the double-layer capacitance could be easily determined in each of the experiments.

In a similar experiment, the Hg/Hg^{2+} reaction in 1 M $HClO_4$ has also been investigated (Sluyters and Oomen [1960]) using IS in the frequency range of 20 Hz to 20 kHz and for concentrations between 2×10^{-6} and 10×10^{-6} mol/cm^3 Hg^{2+}. The results (Figure 1.4.2) show linear behavior in the complex plane with an angle of 45° to the real axis. Such a response is indicative of a distributed element as discussed in the previous section. In this case, the system is under diffusion control as the kinetics of the charge transfer at the electrode–electrolyte interface is much faster than the diffusion of the Hg^{2+} ions in the solution. Solution of the diffusion equation with the appropriate boundary conditions under a small AC perturbation gives the diffusional contribution to the impedance in the complex plane as (see Chapter 2 for a detailed discussion)

$$W = \sigma\omega^{-1/2} - j\sigma\omega^{-1/2} \tag{2}$$

where the impedance W is generally called the Warburg impedance, ω is the angular frequency, j is equal to $(-1)^{1/2}$, and σ is a constant given by

$$\sigma = \frac{RT}{n^2F^2\sqrt{2}}\left[\frac{1}{C_{\mathrm{Hg}_2^{2+}}\left(D_{\mathrm{Hg}_2^{2+}}\right)^{1/2}} + \frac{1}{\left[C_{\mathrm{Hg}}\left(D_{\mathrm{Hg}}\right)^{1/2}\right]}\right] \tag{3}$$

where $D_{\mathrm{Hg}_2^{2+}}$ and D_{Hg} are the diffusivity of mercurous ions in solution and mercury in amalgam, respectively, and the other terms are defined as aforementioned. This impedance is to be added (see Sluyters [1960] and the discussion in Chapter 2) in series with R_2 of Figure 1.3.1d. When the impedance of this circuit is plotted in the complex plane, one obtains a semicircle combined with a straight line at an angle of 45° to the real axis. The line, when extended to the real axis, has an intercept of $R_\infty + R_2 - 2\sigma C_{\mathrm{dl}}$. If $2\sigma C_{\mathrm{dl}}$ is small, as in the present case, the semicircle is suppressed and the product of the imaginary part of W, Im(W), and $\omega^{1/2}$ will be equal to σ at all frequencies.

The experimental results in Figure 1.4.2 are thus consistent with a system under diffusion control. The diffusivity of Hg_2^{2+} ions in solution can be easily calculated (Table 1.4.4) at several different concentrations of Hg_2^{2+} in the solution from the value of σ. No further information can be obtained from this

TABLE 1.4.4 Calculation of Diffusion Coefficient of Hg^{2+} in 1 N $NClO_4$

$C_{Hg_2^{2+}}$ (mol/cm^3)	σ (Ω-s^{-1}/^{2}cm^2)^a	$D_{Hg_2^{2+}}$ (cm^2/s)^b	$R_\infty + R_2$ (Ω-cm^2)
10×10^{-6}	2.09	0.241×10^{-5}	0.190
5	4.10	0.251	0.188
4	4.99	0.264	0.188
3	6.60	0.268	0.195
2	9.73	0.277	0.193

Source: Sluyters and Oomen [1960].

[a] $\sigma = \mathrm{Im}(W)_w^{1/2}$ was found to be independent of frequency within 2%.

[b] $D = [RT(\sigma n^2 F^2 \sqrt{2} C_{Hg_2^{2+}} C_{Hg_2^{2+}})^{-1}]^2$ according to Eq. (3) with $1/[C_{Hg}(D_{Hg})^{-1/2}] \ll 1/[C_{Hg^{2+}}(D_{Hg_2^{2+}})^{1/2}]$, as is the case here with a pure Hg electrode.

data because the time constant associated with the kinetics is too fast to be measured at frequencies below 20 kHz.

The frequency range chosen in the aforementioned experiments was dictated by the limited electronics available in 1960 and the cumbersome experimental approach associated with it, which required that the impedance be measured independently at each frequency. The introduction of automated impedance analysis instruments removes this restriction and allows the experimenter to choose the most appropriate frequency range for a given experiment. This choice should be determined by the nature of the interfaces in the experiment and the time constants that are associated with them. For example, corrosion studies, which often involve a slow aqueous diffusion process, generally have relatively large time constants (on the order of $0.1 - 10$ s), and thus most impedance studies of corroding systems use frequencies between a few millihertz and 100 kHz. On the other hand, studies of solid ionic conductors require higher frequencies to measure the time constant associated with ionic motion (milli- to microseconds), which is generally smaller than those found in aqueous diffusion processes. Thus, frequencies between a few hertz and 15 MHz are most appropriate here.

That is not to say that the frequency range should always be restricted based upon predetermined expectations. In the aforementioned studies, a wider frequency range would probably have allowed a determination of additional information. For the Zn/Zn^{2+} couple, lower frequencies would have allowed the measurement of the diffusivity of zinc ions in the solution. For the study of the Hg/Hg^2 $^+$ couple, the kinetics of the electrochemical reaction at the interface could have been explored by using higher frequencies. Nevertheless, an understanding of the relationship between the time constant in an experiment and the frequencies with which to measure it provides an intelligent starting point in the choice of the most appropriate frequency range.

Another example that illustrates the utility of IS to solid-state chemists is the application of impedance analysis to zirconia–yttria solid electrolytes (Bauerle [1969]). At elevated temperatures solid solution zirconia–yttria compounds are known to be oxygen-ion conductors, which function by transport of oxygen ions through vacancies introduced by the dopant yttria. By examining cells of the form

$$\mathrm{Pt, O_2} \,\big|\, (\mathrm{ZrO_2})_{0.9}\,(\mathrm{Y_2O_3})_{0.1} \,\big|\, \mathrm{O_2, Pt} \tag{4}$$

using IS, admittance plots were obtained (Figure 1.4.3a). The equivalent circuit proposed to fit this data is shown in Figure 1.4.3b. By a careful examination of the effect of the electrode-area-to-sample-length ratio and by measuring the DC conductivity of the samples, the high-frequency semicircle (the one on the right in Figure 1.4.3a) was ascribed to bulk electrolyte behavior, while the low-frequency semicircle (on the left in Figure 1.4.3a) corresponded to the electrode polarization. In the terminology of Figure 1.4.3b, R_1 and C_1 correspond to electrode polarization phenomena, while R_2, R_3, and C_2 describe processes that occur in the bulk of the electrolyte specimen. Furthermore, by varying temperature, oxygen partial pressure, and electrode preparation, the role of each component in the overall conduction

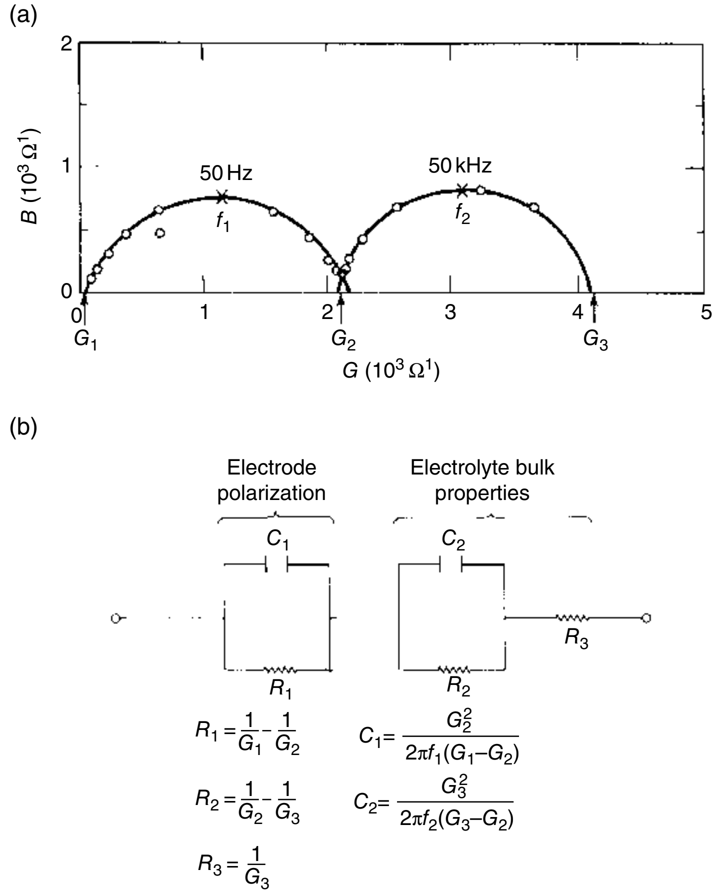

FIGURE 1.4.3 (a) Admittance behavior of the electrochemical cell given in 1.4.4 at 873 K for a specimen with naturally porous electrodes (sputtered Pt). (b) The equivalent circuit for the behavior in part *a* showing the two impedance elements associated with each semicircle. *Source:* Bauerle 1969. Reproduced with permission of Elsevier.

mechanism was determined. In particular, R_1 represents an effective resistance for the electrode reaction:

$$\frac{1}{2}O_{2(g)} + 2e^- = O^{2-}\ (\text{electrolyte}) \tag{5}$$

where C_1 is the double-layer capacitance of the electrode; R_2 is a "constriction" or intergranular resistance corresponding to resistance of conduction across two different grains, primarily due to impurities located there; C_2 is the capacity across the intergranular region; and R_3 is the resistance to conduction within the grains. Electron microprobe studies supported the theory of impurities at the grain boundary. Thus, in a system as electrochemically complex at this, with many different effects interacting, one can still obtain fundamental information about processes occurring at each interface and in the bulk specimen.

This second study illustrates a very important point about IS. Although it is an extremely powerful technique in its own right, the analysis of complicated systems must be correlated with other experimental information to verify that the chosen circuit is physically reasonable. Furthermore, agreement between independently determined experimental values and those determined in a fitting procedure of the complex plane results can only strengthen the IS results and thus should never be overlooked.